

**2023 NDIA MICHIGAN CHAPTER
GROUND VEHICLE SYSTEMS ENGINEERING
AND TECHNOLOGY SYMPOSIUM
AUTONOMY, ARTIFICIAL INTELLIGENCE ROBOTICS TECHNICAL SESSION
AUGUST 15-17, 2023 - NOVI, MICHIGAN**

PHYSICALLY COOPERATING AUTONOMOUS GROUND VEHICLES

Michiel Ashley¹, Davis McMullan¹, Swaminathan Gopalswamy¹

¹Mechanical Engineering, Texas A&M University, College Station, TX

ABSTRACT

Off-road mobility for an individual autonomous ground vehicle (AGV) can be severely limited by extreme environments (such as muddy patches or steep cliffs in off-road terrain). However, when operating as a group, cooperation between the AGVs can be leveraged to overcome such limitations. Traditionally cooperation has been achieved through information sharing, enabling the AGVs to “avoid” the extreme environments. In this paper we propose to achieve such cooperation through physical energy sharing, where the AGVs can “recover” from these environment scenarios. Specifically, we propose the use of a robotic manipulator (RM) that connects a disabled or degraded AGV with an operational AGV. A fleet level controller is proposed. The AGVs and the RM are modeled in Modelica, and integrated with the controller to perform simulations. We demonstrate collaborative movement in two scenarios, namely crossing a muddy patch and climbing a steep cliff. In each scenario the individual vehicle fails to complete the mission when degraded, however the cooperative fleet succeeds, while also enabling the degraded AGV to regain operational status.

Citation: M. Ashley, D. McMullan, S. Gopalswamy, “Physically Cooperating Autonomous Ground Vehicles,” In *Proceedings of the Ground Vehicle Systems Engineering and Technology Symposium (GVSETS)*, NDIA, Novi, MI, Aug. 15-17, 2023.

1. INTRODUCTION

Unmanned autonomous ground vehicles (AGV) are built with the intention to identify, negotiate and avoid challenging terrain including mud, vegetation, steep slopes, and cliffs or other man-made objects. However, misclassifications of upcoming terrain often leads to the AGVs getting stuck, particularly with mud, sand and rubble. The capabilities of a group of unmanned AGVs can

be disproportionately amplified through cooperation. Currently, this cooperation mainly involves sharing digital information between AGVs via appropriate communication methods. However the sharing of digital information does little to return a degraded AGV to an operational state. This paper aims to broaden the scope of cooperation by incorporating energy sharing among AGVs to unlock additional capabilities through such physical collaboration.

We consider extreme environment terrains such as muddy patches (where the wheels will slip and the vehicles get stuck), or steep hills (where the wheels will slip and the vehicles will not be able to climb). These scenarios pose significant mobility challenges for ground vehicles in their ability to maneuver even when manned. The challenges get exacerbated for AGVs, due to the challenges related to dynamic control on such extreme surfaces, including the lack of other means to maneuver that would have been available if human support could be leveraged, such as the use of tethers around objects anchored to solid ground to pull the vehicles across difficult terrain.

The paper intends to develop a solution that addresses scenarios involving extreme environment terrains.

1.1 Related Work

A partial solution that addresses slippery terrain is the use of higher traction-force wheels, either through higher friction or specialized wheel interfaces [1]. However such solutions are not effective when the slippery surfaces also present a steep grade. Another partial solution to such problems considers a fleet of vehicles working in concert, using tethers that link multiple vehicles (or different parts of reconfigurable vehicles) where the tethers provide support, power and communication capabilities [2]. While these tethers have potential to improve the collective capability of the fleet, they still have fundamental limitations arising from the fact that these tethers can only support tension, and so only a subset of possible maneuvers can be supported by these “soft” tethers. In particular, vehicles can only go down steep craters using soft tethers, but cannot go up steep craters. Similarly, stuck vehicles can only be pulled back from stable ground, but cannot be pushed out on to stable ground. Alternatively, “hard” tethers, which are essentially robotic manipulator connections between vehicles, can achieve both pushing and pulling. Hard tethers can be used in addition to, or independent of, any

higher traction-force wheel solutions.

In [3-4] technologies for coordinated maneuvers between a heterogeneous team of autonomous ground and air vehicles are being developed. These approaches are focused on information sharing across the vehicles using wireless communications, and clearly demonstrate the value of cooperation, especially in unstructured and potentially adversarial environments. For example, distributed multi-agent tracking approaches are developed in [5-6] that demonstrate how collaboration can be leveraged to maximize tracking over diverse objects. In [7] the concept of Hard Platooning is being developed. The fundamental mechanism is an articulated connection between a follow-vehicle and a lead-vehicle, with the intent that the follow-vehicle be controlled such that the articulated connection is maintained to be as close to no-load conditions as possible, even as the lead-vehicle performs its own motion. The concept here also has an articulated connection. However this is the “inverse” of the Hard Platooning concept, where the follow-vehicle will be controlled such that the articulated connection is loaded to ensure the lead vehicle performs a desired motion.

Previous work on physical cooperating AGV’s utilizes an unactuated four-bar linkage like mechanism to connect two vehicles [8-10]. The system has three links in total, connected with pin-joints. The link immediately connected to each vehicle can be latched in a vertical position to create a lever arm that allows one AGV in the two vehicle system to partially lift off of the ground with the wheels of one axle (or one end of a tracked vehicle) to remain in contact with the ground. This system utilizes a de-centralized control strategy where neither AGV communicates with the other. The authors use Jacobian linearization to design controllers, with the input being wheel torque. The controlled output is pitch angle of the AGV crossing the gap and inertial position of the supporting AGV. This system was applied to a gap crossing scenario, where the leading AGV was tilted and placed across

the gap, which then pulled the following AGV across. This system can only cross gaps that have a width less than the AGV's wheelbase. The researchers list several potential advantages of this system, such as cost-effectiveness, ability to retrofit the system onto existing robots, and a strong physical connection. However, the non-actuated linkage challenges the systems capability to push the leading AGV through or up demanding terrain because the linkage folds at the pin joints. The de-centralized control strategy also limits the capabilities of the system by not allowing the AGVs to fully cooperate and utilize the full range of their mobility. The higher level decision making of when to actuate the locking of the linkage would also have to be done through cooperation.

Other related works involve snake-like robotics, such as in these reviews [11-12], and modular single-axle ground vehicle systems such as electric steerable units that can be connected in pairs to make a four wheel vehicle or connected like trailers to existing ground vehicles [13]. Snake-like robots have multiple power unit segments cooperating together to achieve the goal of improved mobility, they can readily navigate difficult terrain such as mud and steep inclines but they are purpose built and lack significant payload carrying capacity. Similarly the electric single-axle modules are also purpose built and unless they are already connected they cannot support the recovery of a degraded vehicle.

1.2 Proposed Concept

The primary contribution of this paper is the proposed concept for cooperative behavior in extreme environments. Here, physical energy sharing is enabled through a robotic connector that links a disabled AGV with an operational one. The connector is similar to a robotic manipulator (RM) in that it has the appropriate actuated degrees of freedom to fold and extend out to connect one AGV to another. The RM can be a multi-use component whose capability encompasses both environment

manipulation and physical cooperation. Some of the RM will have the ability to be locked, so as to enable vehicle-to-vehicle transfer of large forces and torques while isolating the embedded joint actuators that are not rated for high forces and torques. The RM will have sufficient degrees of freedom to allow for relative motion of the vehicles, as required for traversing difficult off-road terrain.

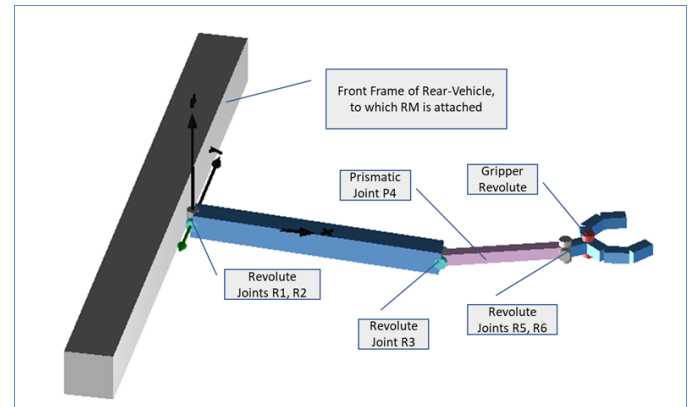


Figure 1: Example embodiment of a RM: expanded configuration

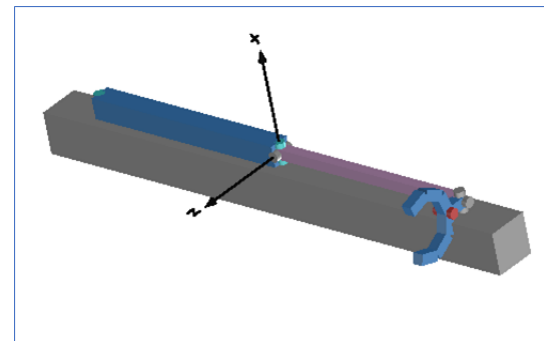


Figure 2: Example embodiment of a RM: collapsed configuration

Figures 1 and 2 show one example embodiment of the proposed concept for the RM.

While there are many interesting dynamic control issues to be considered in the actuation of the RM to connect the leader and follower vehicle, since it is a relatively solved problem, we do not focus on it in this paper. Instead we assume that RM is already connected and then develop a control strategy

to guide the vehicles with a fleet perspective that engenders cooperative behavior.

We demonstrate the concept by modeling the system dynamics in the declarative language Modelica, and simulating the models in two different scenarios: (i) two vehicles traversing a muddy patch that does not provide the required traction and (ii) two vehicles traversing a steep cliff, which again requires higher than normal traction to navigate. We demonstrate how a cooperative behavior emerges based on our proposed control strategy, where the vehicles pull and push each other to move the fleet collectively forward.

2 PCR MODEL

While the proposed concept is general and can be applied to multiple vehicles that are connected together, we will consider a fleet of just two vehicles, denoted by v_i with the subscript $i \in \{1, 2\}$. Without loss of generality, we will assume v_2 is following v_1 .

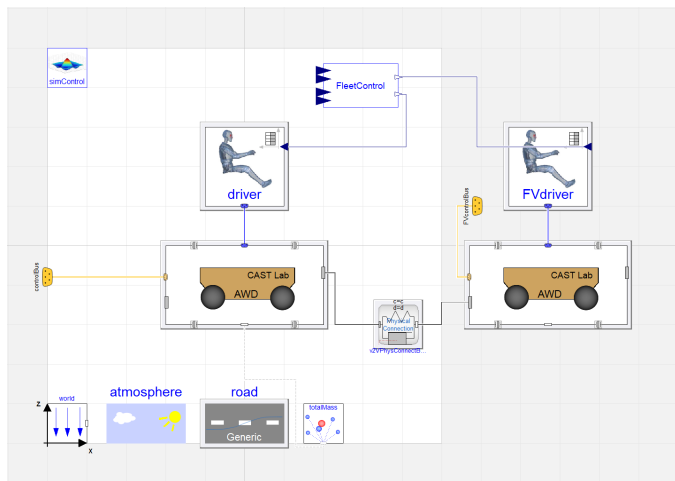


Figure 3: Modelica AGV fleet model top level

Figure 3 shows the top-level of the fleet model which is developed using the commercial Modelica library Vehicle Systems Modelling and Analysis (VeSyMA). The atmosphere conditions are set to no wind and the model does not depend on temperature. The road model is defined by

a .mat file that specifies the surface points and corresponding friction. The driver and FVdriver subsystems are VeSyMA OpenLoop models with the externalAcceleratorInput flag set to true.

The AGV created in simulation is a four-wheeled vehicle driven by a single electric motor. This vehicle model was created by extending from the Automotive.RearWheelDrive.ExecutiveElectric class and redeclaring the powertrain subsystem with a custom model. The left front and rear wheels are geared together such that they rotate with the same angular velocity and likewise for the right two wheels of the vehicle. This powertrain is created by extending from the Drivelines.RearWheelDrive1D class, adding a connector from the right side output of the differential to the front right wheel and adding a corresponding connector for the front left wheel. The CAD visualization was replaced with a custom 4 wheel simple AGV model. Lastly fixed translations and multibody frame interfaces from the Modelica Standard Library were added to the front and rear of the vehicle for RM connection points. All other modifiers to the vehicle and powertrain subsystem are shown in Table 1.

Table 1: Model Parameters

Parameter	Value
AGV mass	650 kg
Body center of mass r_{CM}	(-1, 0, 0.25) m
Body inertia I_{11}, I_{22}, I_{33}	500, 600, 625 kg m ²
Wheel size	265/70R19.5
Wheel base	2.1m
Track width	1.4m
RM hitch dist above chassis	0.75 m
RM length	5m
RM stiffness	6 kN/m
RM damping	30 kN s/m

The suspension is rigid but the tires include vertical dynamics. For each tire a contact point location is calculated by interpolating the ground

surface points. This contact point is used to calculate the normal force, tractive force and rolling resistance on each tire. The tires are allowed to loose contact with the ground. The tractive force generated at the tire-road interface is based on a linear model and is dependent on the normal force exerted on the tire. Rolling resistance is present even when the ground friction is zero, and this term is what brings the AGV to a stop when it is in the mud. The RM is modeled as a stiff spring and is connected to the bumpers of the AGVs through ball joints.

3 PCR CONTROL

The control objective is for the fleet to travel together at a desired velocity $v_{f,d}$. This is achieved by commanding appropriate torques τ_i from the motors of the two vehicles of the fleet.

We define two *fleet level* variables, the fleet average velocity v_f and the fleet torque τ_f as below:

$$\begin{aligned} v_f &= (v_1 + v_2)/2 \\ \tau_f &= \tau_1 + \tau_2 \end{aligned} \quad (1)$$

A simple closed loop PI controller is utilized to determine the fleet torque as below:

$$\tau_f = PI(v_{f,d} - v_f) \quad (2)$$

To calculate the motor torques at the individual vehicles, we first need to identify which vehicle is in “degraded” status. Towards this, we consider the tire slip ratio λ defined as below:

$$\lambda = \frac{v - r\omega}{\max(v, \epsilon_\lambda)} \quad (3)$$

where ϵ_λ is a tuned velocity threshold.

Define λ_{max} as the maximum tire slip ratio before we deem the particular vehicle is in degraded status:

$$\text{vehicle status} = \begin{cases} \text{operational} & \lambda \leq \lambda_{max} \\ \text{degraded} & \lambda > \lambda_{max} \end{cases} \quad (4)$$

Also define the following variables:

$$\begin{aligned} \tau^n &= \tau_f/2 \\ \tau^d &= \tau^n e^{\gamma(\lambda_{max}-\lambda)} \\ \tau^o &= \tau^n (2 - e^{\gamma(\lambda_{max}-\lambda)}) \end{aligned} \quad (5)$$

Here γ is a calibratable constant that determines how aggressively traction limits are to be applied.

Then individual motor torques will be determined from:

$$[\tau_1, \tau_2] = \begin{cases} [\tau^n, \tau^n] & \text{AGVs 1 and 2 operational} \\ [\tau^o, \tau^d] & \text{AGV 1 operational, 2 degraded} \\ [\tau^d, \tau^o] & \text{AGV 1 degraded, 2 operational} \\ [\tau^d, \tau^d] & \text{AGVs 1 and 2 degraded} \end{cases} \quad (6)$$

The actual motor torque commands are provided as a percentage of maximum torque, $\tau_{i,cmd} = \tau_i/\tau_{i,max}(\omega_i)$

In the case when both the vehicles are degraded, the control will not yield a satisfactory performance of the vehicles with respect to desired vehicle (fleet) speed. However it will prevent excessive slip at the wheels.

4. SIMULATION EXPERIMENT SETUP

Two test scenarios are created to demonstrate the fleet level cooperation. The first is on flat ground with a section of mud represented by a coefficient of friction equal to zero. The rest of the ground in this scenario has a coefficient of friction equal to one. The mud pit has a length of 5m, which is the same length of the RM. The second scenario is a steep incline with friction characteristics consistent with that of loose dirt, $\mu = 0.75$. The steep incline has a maximum slope of 70° and a 6 m overall increase in elevation. Additional simulation parameters are presented in table 2, where the tire rolling resistance coefficients are passed as modifiers into the tire force subsystem.

Table 2: Simulation Parameters

	Mud	Incline
Tire const roll resistance	0.6	0.2
Tire linear roll resistance	0.6	0.2
Ground friction μ	$\mu \in \{0, 1\}$	0.75
Max slip λ_{max}	1	1
Traction limit coef γ	5	5
Velocity target	3 m/s	3 m/s

5 RESULTS

First we show that a single AGV is unable to negotiate either scenario on its own, coasting to a stop in the mud and sliding down the steep incline. Then the fleet control method from equation (6) is implemented on both the mud pit and steep incline scenarios.

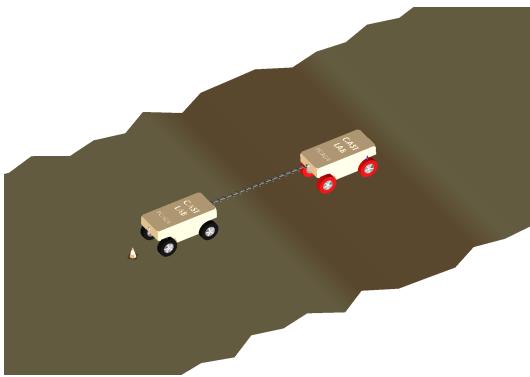


Figure 4: Test scenario: mud pit

5.1. Mud Pit Scenario

Figure 4 shows an image of the fleet crossing the mud pit. The darker color ground is the mud pit and is where the friction is zero. The wheels are animated in the color red when they are slipping with a ratio greater than 1 and the wheels become yellow if they lose contact with the ground.

First we examine the results of a single AGV *without PCR* attempting to cross the mud pit. The results are shown in figure 5. Initially the torque controller successfully brings the vehicle speed up to the 3 m/s setpoint. However once the vehicle enters the mud pit at 8 seconds, the reduced tractive

friction coefficient results in reduced tractive force. Simultaneously the mud offers sufficient rolling resistance resulting in the vehicle coming to a stop. The tire slip coefficient λ , from equation (3), crosses the $\lambda_{max} = 1$ threshold and the vehicle becomes degraded. The single AGV is also utilizing the same traction controller as the fleet but without an operational vehicle to share the torque demand with. The traction controller rapidly decreases the motor torque output to near zero to prevent further degradation until the about 12 seconds when the wheel slip is near the threshold again. With no way to generate a tractive force the AGV remains stuck in the mud.

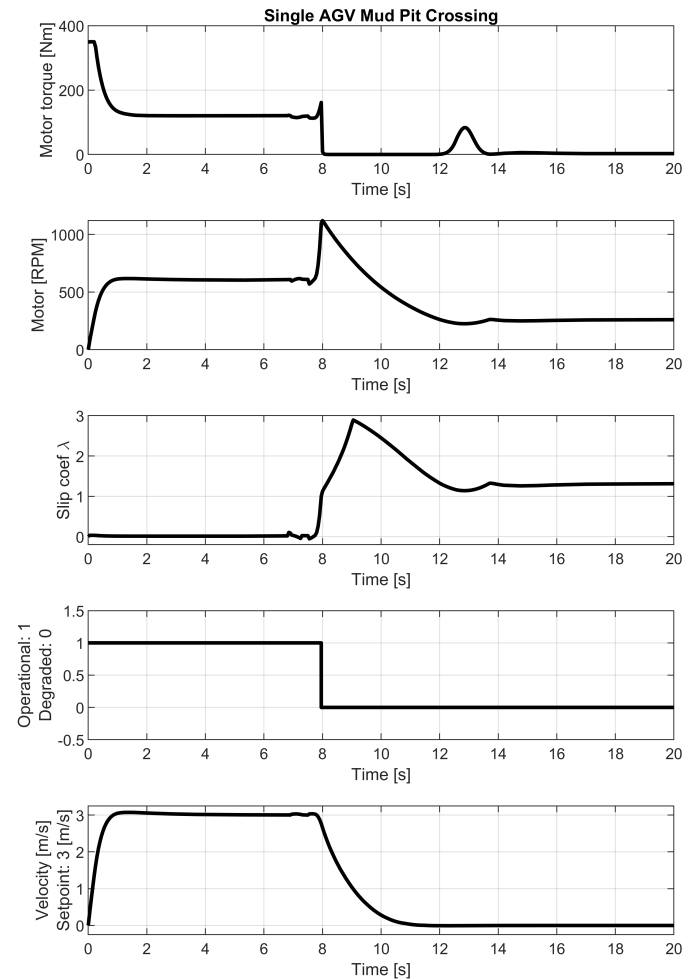


Figure 5: Single AGV failing to traverse mud pit

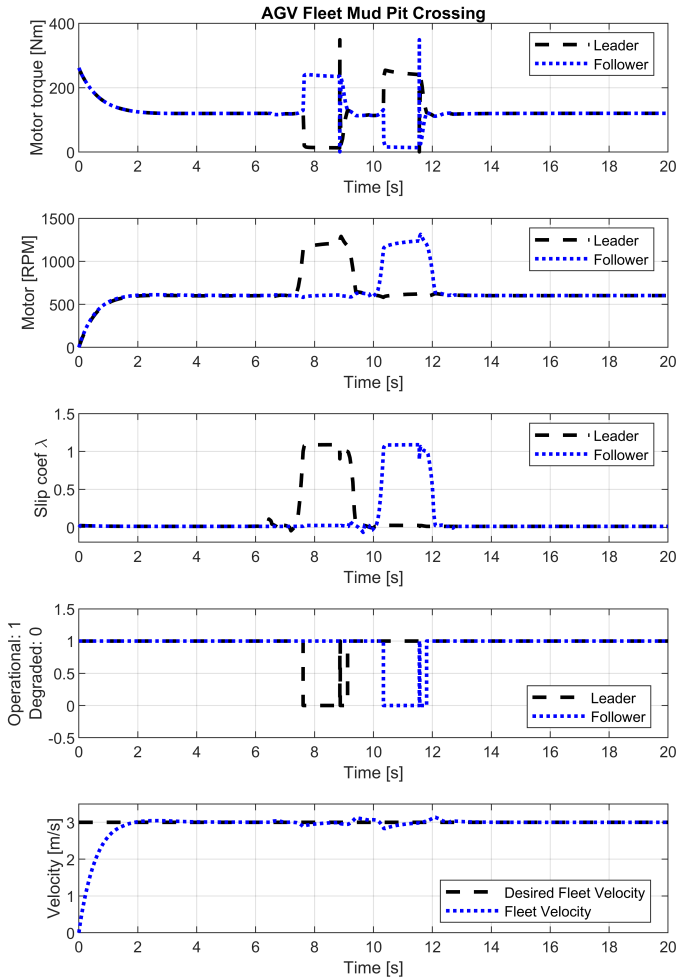


Figure 6: Mud pit test scenario - recovery using PCR with operational vehicle increasing its torque

Now we consider the system *with PCR*. In figure 6 the lead vehicle becomes degraded immediately upon entering the mud pit at 6 seconds when the slip coefficient becomes greater than λ_{max} . The length of the RM is such that neither AGV is in the mud at the same time and correspondingly only one AGV is degraded at a time - leaving the operational AGV to compensate for the degraded AGV. Initially when both AGVs are in an operational state the motor torques are equal however when the lead AGV enters the mud pit the fleet controller reduces its torque following equation (5-6) and the follower is made to compensate by doubling its torque from 7.5 to

9 seconds to maintain the fleet's objective velocity. Likewise, when the follower enters the mud the leader doubles its motor torque from 10.5 to 12 seconds.

An increase in velocity can be seen at 9 and 11.5 seconds corresponding to the moment when each of the AGVs are pushed or pulled onto solid ground to regain traction and transition from being degraded to operational. During the degraded state the fleet controller limited the motor torque to ensure that the AGV does not continue to excessively spin up the wheels and exacerbate the degradation. However the wheels continue to spin at a reduced rate and upon regaining traction they cause a spike in torque and brief increase in velocity. The mud pit scenario shows the systems ability to adapt from each AGV being degraded and operational.

5.2. Steep Incline Scenario

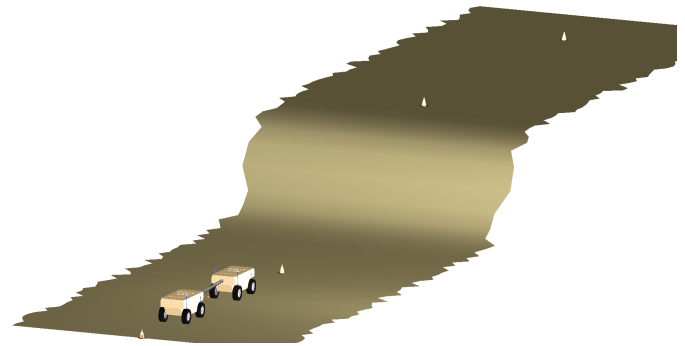


Figure 7: Test scenario: 70° max slope steep incline

In figure 8 the results of a single AGV failing to traverse the 70° hill are presented. Unlike the solid ground in the mud scenario, which has a friction coefficient of $\mu = 1$, the ground friction for this scenario is $\mu = 0.75$. This causes a higher initial wheel slip as the vehicle accelerates from zero velocity under the maximum commanded motor torque. The controller is still able to maintain the velocity setpoint of 3 m/s on the flat ground. However, when the vehicle reaches the hill it becomes degraded and slides back down.

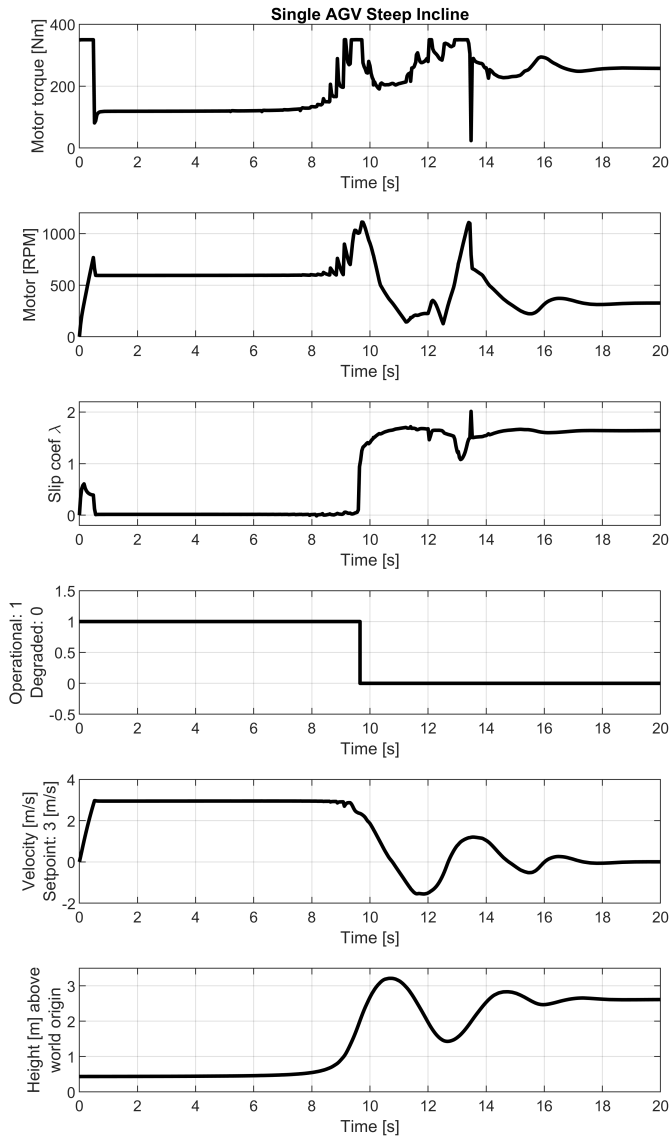


Figure 8: Single AGV failing to traverse steep incline

The vehicle’s momentum and limited tractive force initially carrier it up to 3m which is half way up the 6m hill. The vehicle remains degraded after reaching the hill and the traction controller correspondingly reduces the motor torque to prevent excessive slip but the vehicle remains unable to climb.

Now we consider the system *with PCR*. From figure 9 both AGVs initially have the same torque output and are each carrying their own weight. When they reach the hill with the maximum slope of 70° the

motor torque outputs increase and saturate with the lead vehicle making it up to about 5m at 7.5 seconds before it becomes degraded.

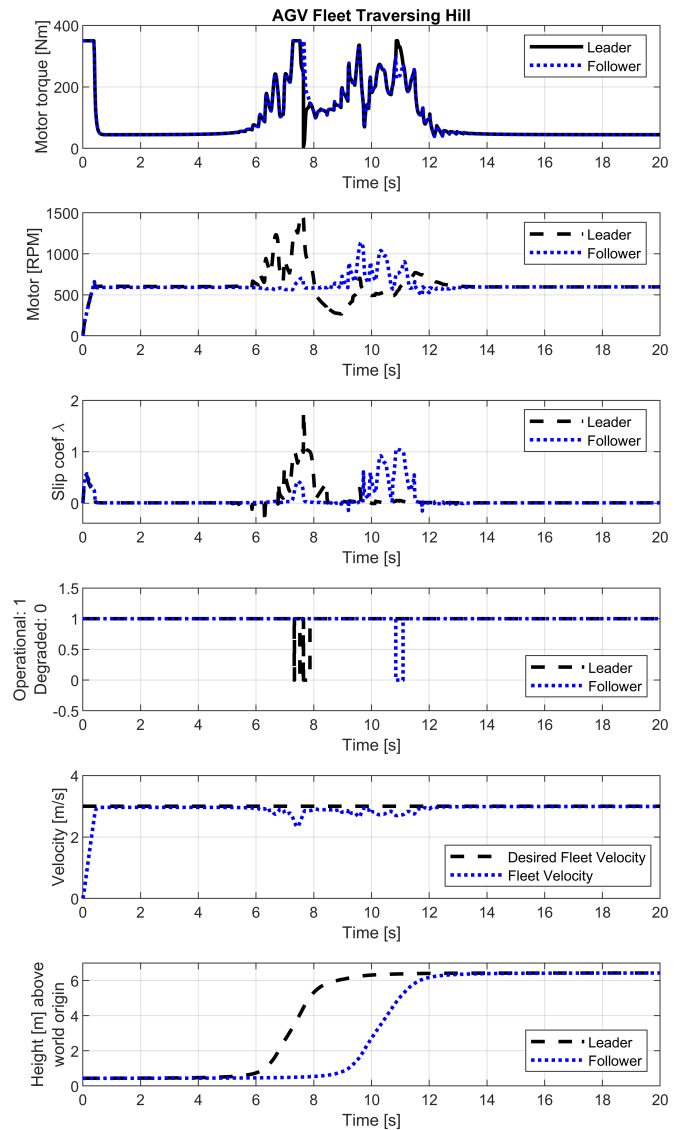


Figure 9: Steep incline test scenario - recovery using PCR to successfully climb

At 7.5 seconds the fleet controller limits the leader’s motor torque while the follower’s is saturated at the maximum. At the same instance there is a increase in the follower’s slip coefficient to about $\lambda = 0.4$, which is small given that the torque command is saturated. This is because the weight of the lead vehicle is

transmitted through the RM which is increasing the tire normal force and decreasing the the tire's tendency to slip. While on the incline the tire normal force is significantly reduced and the tire is more readily able to slip. However, unlike in the mud pit, the fleet controller recovers from the degraded state quickly by reducing the input torque for less than one second.

The motor RPM is also increased for the AGV that is climbing the incline as it must travel a further distance. From the bottom subplot in figure 9 the leader starts climbing the incline around 5.5 seconds and the motor RPM simultaneously begins to increase to maintain the fleet velocity, however the slip coefficient does not increase until 6.5 seconds. Motor RPM alone cannot indicate a degraded state.

5.3. Sensitivity Study for Steep Incline Scenario

In section 5.1 and 5.2 specific examples were given to demonstrate the fleet's physical cooperation capabilities. Now we test the system on variations of the steep incline scenario by examining the sensitivity to different ground friction coefficients and different steep inclines. First we test the response to different ground friction by holding all other parameter's constant and using the 70° maximum slope road with an elevation change of 6m. The results are shown in figure 10 where, to increase readability, all of the subplots except the velocity is data from the following vehicle. The velocity subplot is the fleet velocity. Each of the 4 presented runs have a friction coefficient less than the scenario presented in section 5.2 which causes the vehicles to initially become degraded as the fleet accelerates from zero speed.

Unlike the simulation in section 5.2, the following AGV becomes degraded when the lead vehicle initially reaches the hill. For friction coefficients $\mu = 0.5$ and $\mu = 0.6$ the follower regains operational status after the initial climbing by the leader and again loses it once it is on the incline.

However, for these friction coefficients the fleet is still able to successfully climb the hill.

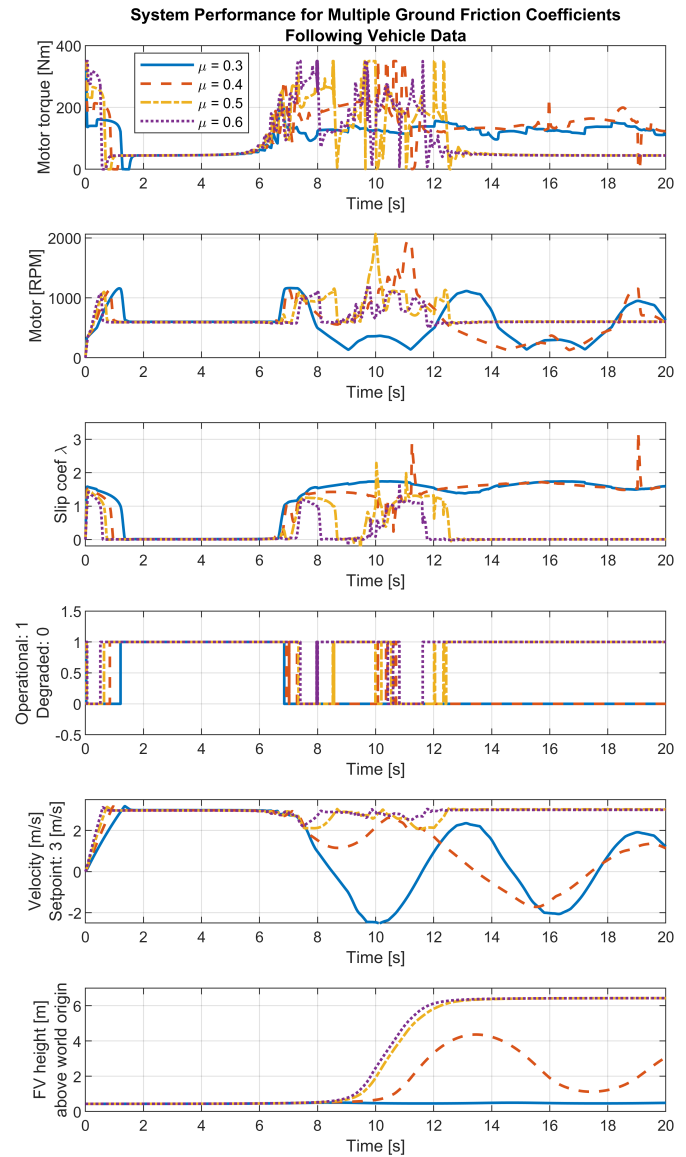


Figure 10: System sensitivity to different ground friction coefficients on the 70° max slope incline

From equation (5-6) we expect undesirable fleet performance with the system no longer tracking the velocity control objective when both AGVs are degraded because both motor torques are reduced. However, a tractive force is still being generated and the fleet is able to climb the hill. This demonstrates

the system’s ability to get out of scenarios even when both vehicles are degraded but can still generate a tractive force.

For $\mu = 0.4$, the leading AGC makes it on top of the hill but the follower does not. For $\mu = 0.3$ neither the leader or follower can make it up the hill. In both of these runs the velocity becomes negative as the fleet slides down the hill.

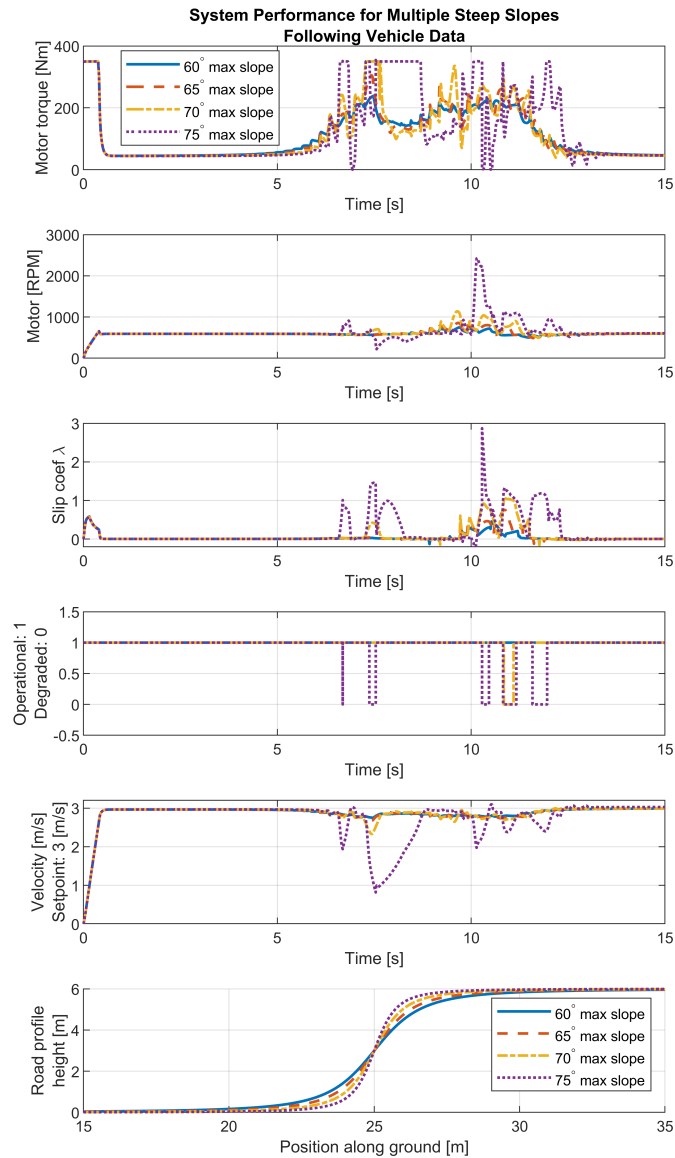


Figure 11: System sensitivity to different inclines

Next we test the physically cooperating robot fleet to different road profiles as shown in figure

11. The bottom subplot shows the different road profiles and has a horizontal axis different than the other subplots. In each of the 4 presented runs the coefficient of friction is $\mu = 0.75$. For a road profile with a maximum slope of 60° neither vehicle becomes degraded and the fleet climbs the hill while simultaneously maintaining the velocity objective. The 65° and 70° runs are successful. Once the road profile reaches a maximum slope of 75° the fleet begins to experience more degradation and significant decreases in velocity, down to 1 m/s at about 7.5 seconds, when the leader first contacts the hill. In this run the follower’s motor torque saturates at its max as the leader is climbing the hill from about 7-8 seconds but with the weight of the leader transmitted to the follower the wheel slip remains below the threshold. However the fleet still manages to navigate the cliff obstacle.

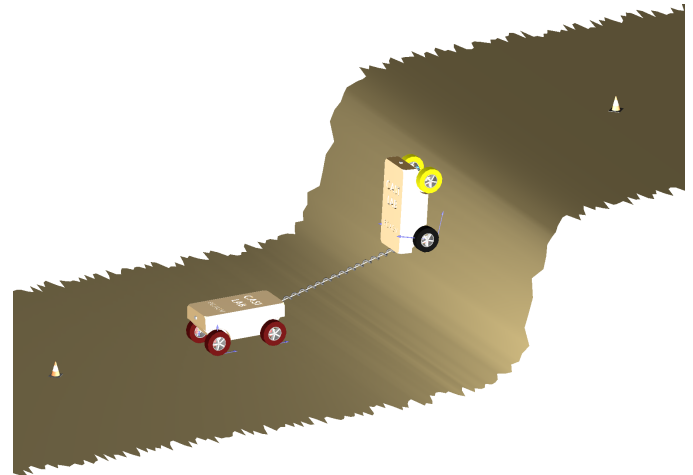


Figure 12: Moments before the lead vehicle flips over on the 80° maximum slope incline

A simulation run with an 80° slope was performed but the leader flipped over - an image is shown in figure 12. This demonstrates the importance of choosing a connection point location for the RM. A connection point that is on a lever arm up from the bumper may not be an embodiment that works well in all scenarios. In the case of the 80° slope it would make more sense for the connection

point to be inside the wheel base so that no moment is generated that induces a tendency for the vehicle to flip over and the vehicle is only pressed against the cliff.

6 CONCLUSIONS

In this paper we proposed a mechanization that would allow for physical energy sharing between autonomous vehicles, along with a control algorithm that results in an emergent collaborative behavior. The degraded vehicle adapts its strategy to minimize the extend of degradation, while the operational vehicle steps in to compensate for the degraded vehicle. This is achieved through a few steps:

- A fleet level mission is defined. In this specific example, a fleet level desired vehicle speed is defined.
- A composite control that closes the loop on the deviation between the fleet level desired vehicle speed and the average fleet speed is performed.
- A definition of degradation is defined. In the specific examples, the tire slip ratio is used as the metric for this.
- Individual vehicle controls are derived from the composite control, that accommodates the degradation status of the vehicle. Individual vehicle degradation is arrested without compromising on fleet control requirements - as long as at least one vehicle is operational.

We demonstrate the above capability through numerical simulations on two scenarios - (i) traversal across a muddy patch of off-road terrain, and (ii) climbing over a steep hill.

The current work focused on longitudinal dynamics only. Future work will extend the approach to include both longitudinal and lateral dynamics. Pushing on a degraded vehicle through a long robot manipulator may induce jack-knifing

so the following methods will be studied: (1) adding a 2nd RM to connect at the widest points of the vehicles (2) having the ability to apply a torque at the RM end-effector through embedded actuators or (3) steering control by the operational vehicle. Future work will also include the further impact of different suspension characteristics and the methodology developed for 2 vehicles will be generalized to multi-vehicle systems. We will validate the above approach by building prototypes and performing field experiments.

7. REFERENCES

- [1] M. Russo, M. Ceccarelli, "A Survey on Mechanical Solutions for Hybrid Mobile Robots", *Robotics* 2020, 9, 32. <https://doi.org/10.3390/robotics9020032>.
- [2] P. McGarey, W. Reid and I. Nesnas, "Towards Articulated Mobility and Efficient Docking for the DuAxel Tethered Robot System", 2019 IEEE Aerospace Conference, 2019, pp. 1-9, doi:10.1109/AERO.2019.8741573
- [3] S. Gopalswamy, et.al, "Air-Ground Coordination", Cooperative Agreement Research with Army Research Labs (2019-2021)
- [4] S. Gopalswamy, et.al., "Robust Threat Detection", Cooperative Agreement Research with Army Research Labs (2019-ongoing)
- [5] T. Li, L. W. Krakow and S. Gopalswamy, "Optimizing Consensus-based Multi-target Tracking with Multiagent Rollout Control Policies," 2021 IEEE Conference on Control Technology and Applications (CCTA), 2021, pp. 131-137, doi: 10.1109/CCTA48906.2021.9658603.
- [6] T. Li, L. W. Krakow, and S. Gopalswamy. "SMA-NBO: A Sequential Multi-Agent Planning with Nominal Belief-State Optimization

- in Target Tracking.” arXiv preprint arXiv:2203.01507 (2022), presented at IROS 2022.
- therein.” U.S. Patent No. 11,186,314. 30 Nov. 2021.
- [7] D. J. Franklin, M. Ashley and S. Gopalswamy, “Application of Nonlinear Control for Hard Truck Platooning,” 2022 International Conference on Connected Vehicle and Expo (ICCVE), 2022, pp. 1-6, doi: 10.1109/ICCVE52871.2022.9742997.
- [8] A. Deshpande and J. Luntz, “Decentralized control for a team of physically cooperating robots,” Proceedings 2003 IEEE/RSJ International Conference on Intelligent Robots and Systems (IROS 2003) (Cat. No.03CH37453), Las Vegas, NV, USA, 2003, pp. 1757-1762 vol.2, doi: 10.1109/IROS.2003.1248898.
- [9] A. Deshpande and J. Luntz, “Behaviors for Physical Cooperation Between Robots for Mobility Improvement”, *Autonomous Robots* (2007), 23(4), 259-274. doi: 10.1007/s10514-007-9044-9
- [10] A. Deshpande and J. Luntz, “A methodology for design and analysis of cooperative behaviors with mobile robots” Springer, *Autonomous Robots* (2009) 27: 261–276, doi: 10.1007/s10514-009-9125-z
- [11] K. Y. Pettersen, “Snake robots” *Annual Reviews in Control*, Volume 44, 2017, Pages 19-44, ISSN 1367-5788, <https://doi.org/10.1016/j.arcontrol.2017.09.006>.
- [12] J. Liu, Y. Tong, J. Liu, “Review of snake robots in constrained environments” *Robotics and Autonomous Systems*, Volume 141, 2021, 103785, ISSN 0921-8890, <https://doi.org/10.1016/j.robot.2021.103785>.
- [13] A. B. Shoshan, and A. Engel. “Articulated vehicle assembly and articulation system for use